UNITED STATES DEPARTMENT OF THE INTERIOR

GEOLOGICAL SURVEY

PALEOMAGNETISM OF TRIASSIC RED BEDS AND BASALT IN THE CHULITNA TERRANE, SOUTH-CENTRAL ALASKA

By

J. W. Hillhouse and S. Grommé

Open-File Report

80-368

This report is preliminary and
has not been edited or reviewed
for conformity with Geological
Survey standards or nomenclature

Abstract

The Chulitna terrane in south-central Alaska is an elongate belt of highly deformed Devonian ophiolite overlain by upper Paleozoic to lower Mesozoic volcanic and sedimentary rocks. Paleomagnetic measurements were made in upper Triassic redbeds and metabasalt of the terrane to determine its paleolatitude. In general, the redbeds have stable, single-component magnetizations, as indicated by thermal demagnetization to 650°C. However, correcting the magnetic directions for tilt of the bedding markedly increases the directional dispersion between site means, indicating the rocks were magnetized after they were folded. The Chulitna metabasalts have multicomponent magnetizations which preclude calculation of a meaningful average direction. The upper Triassic paleolatitude of the Chulitna terrane cannot be determined because the stable remanent magnetism of the redbeds and basalts originated long after deposition.

Introduction

Pre-Cenozoic rocks of the upper Chulitna District are a key element of the tectonic accretion of south-central Alaska. The district contains a unique assemblage of upper Paleozoic and Triassic volcanic and sedimentary rocks that were deposited on Devonian ophiolite. Uniqueness of the assemblage is underscored by the occurrence of early Triassic limestone and upper Triassic redbeds found nowhere else in Alaska.

The ophiolite and the overlying rocks associated with it define the Chulitna terrane (Jones and others, 1979). Chulitna is one member of a family of fault-bounded terranes which make up southern Alaska. Each terrane has a distinct stratigraphy, history of metamorphism, and structural style which set it apart from its neighbors. For example, the Triassic depositional history of the Chulitna terrane is unlike the history inferred in nearby Wrangellia, a large terrane whose northern boundary lies a short distance southeast of Chulitna (Jones and others, 1977).

Although the Chulitna Terrane covers only a small area, its location between Wrangellia and large terranes to the west makes it an important part of the tectonic history. Paleomagnetic evidence indicates Wrangellia is an exotic terrane that has moved northward more than 3000 km relative to the North American craton sometime between the upper Triassic and the late Cretaceous (Hillhouse, 1977). The anomalously low paleolatitude of Wrangellia was determined from the upper Triassic Nikolai Greenstone. As reported here, we sampled upper Triassic rocks in the Chulitna terrane to determine its paleolatitude for comparison with the exotic paleoposition of Wrangellia.

The Chulitna terrane possesses rock types which should have been ideal for the paleomagnetic study. In addition to well-dated basalts, the terrane includes redbeds, a rock type used extensively in paleomagnetic studies. Unfortunately, our objectives were not realized in this study because the remanent magnetization in Chulitna basalts and redbeds originated long after the rocks were deposited.

Geologic Setting

The Chulitna District is on the north side of the Chulitna River in the central Alaska Range (Fig. 1). Paleozoic and Mesozoic rocks in the district are arranged in parallel terranes that generally trend 30°-40° northeast. Geologic descriptions of these terranes and a review of previous work in the area are presented by Jones and others (1979).

The object of our paleomagnetic study, the Chulitna terrane, has a well-dated stratigraphy. The oldest rocks make up an ophiolitic sequence that includes serpentinite in fault contact with gabbro, diabase, pillow basalt, and red radiolarian chert of Devonian age. Upper Paleozoic rocks composed of volcanic conglomerate, sandstone, chert, argillite, and limestone lie structurally above the ophiolite. In the northeastern part of the district, Permian limestone is in depositional contact with upper Triassic redbeds. Red chert pebbles in the redbeds were probably derived from the ophiolite. In the northwestern part of the district, a distinctive upper Triassic sequence of pillow basalt interbedded with gray limestone underlies the redbeds, but the base of the basalt--limestone unit is not exposed. Upper Triassic redbeds in the central area of the terrane are gradationally overlain by brown marine sandstone and siltstone as young as Early Jurassic. The youngest unit of the Chulitna terrane consists of dark gray argillite, gray to black chert, and thin beds of limestone of late Jurassic to Early Cretaceous age.

Structurally, the terrane consists of subparallel fault-bounded blocks containing many small folds. The favored interpretation of the overall structure is a stack of thrust sheets folded into a complex synform overturned to the southeast (Jones and others, 1979). The Chulitna terrane appears to have been thrust over Cretaceous flysch, then the whole package was redeformed into southeastward verging folds. This interpretation assumes the Chulitna assemblage of rocks is rootless and very thin, and is underlain structurally by Cretaceous flysch. The low metamorphic grade of the Chulitna terrane indicates deformation occurred at relatively shallow depths in the crust. Secondary mineral assemblages in the Triassic pillow basalts are of lower greenschist facies; original textures are preserved in the basalts and redbeds.

Paleomagnetic Sampling and Results

Oriented cores were collected with a portable drill at 5 localities in the northern half of the Chulitna terrane (Figure 1). All sample localities in the rugged area were reached by helicopter. The geologic settings and paleomagnetic results of each locality are presented in the following subsections (Table 1).

Long Creek: Sites 1-4

Redbeds exposed in Long Creek lie depositionally on Permian argillite; the uppermost redbeds are faulted against Permian andesitic tuff. The paleomagnetic samples consist of 63 cores distributed in four clusters (each spans about 20 m of section) separated by faults. Total stratigraphic thickness spanned by the paleomagnetic collection is about 200 meters. The redbeds dip steeply 45^{o}-90^{o} northwest; variations in bedding attitude were observed across the faults.

The redbeds consist of brick-red sandy and silty mudstone interbedded with pebble stringers. Pebbles, which range from 1 cm up to 10 cm in diameter, consist predominately of red chert and lesser amounts of quartzite and metasedimentary rocks. The sandy matrix has a volcaniclastic composition. Locally, calcite veins fill cracks in the redbeds. Paleomagnetic sampling was concentrated in silty and sandy beds, but a number of cores contain pebbles up to 1 cm in diameter.

Paleomagnetic results from Long Creek

Natural remanent magnetizations (NRM) measured from each site have intensities ranging from 10^{-3}-10^{-5} emu/cm^3 and show very little directional dispersion. Before application of the tilt correction, the four sites have statistically identical mean directions centered on (I=85°, D=225°). Each sample was thermally demagnetized at progressive temperature steps ranging from 200°C to 670°C. Vector diagrams derived from the thermal experiments indicate a single component of magnetization stable up to 650°C (Fig. 2). The high blocking temperature indicates much of the remanence is carried by hematite, but magnetite may be responsible for some of the remanence with blocking temperatures below 580°C. The presence of magnetite has not been confirmed by petrography or magnetic tests.

Cores containing coarse-grained sand and pebbles have magnetic directions identical to the siltstone cores, so the magnetization is probably of post-depositional origin. This conclusion is affirmed by a negative fold test. Correcting the results for tilt of the bedding markedly increases the directional dispersion between sites, indicating the magnetization was acquired after the rocks were faulted and folded (Fig. 3A).

Blind Creek: Sites 5-7

Two redbed sections (Sites 5 and 6) and one metabasalt flow (Site 7) were sampled near Blind Creek. Site 5 consists of 8 cores spanning 2 meters of red chert-pebble conglomerate. Site 6 is 40 m downslope from Site 5, but faulting obscures the stratigraphic relations. Site 6 spans stratigraphically 8 m of red volcaniclastic sandstone and is represented by 8 cores. A one-m-thick metabasalt flow (Site 7), that underlies the redbeds of Site 6, is represented by 8 cores. The Lower Triassic ammonite locality #19 described by Jones and others (1979) lies a few meters beneath our paleomagnetic sites. However, the overlying redbeds are interbedded with limestone boulders containing upper Triassic fossils, indicating millions of years are not represented in the thin Triassic sequence.

Paleomagnetic results from Blind Creek

NRM's from the two redbed sites cluster with moderate dispersion about a steep, downward direction in the northwest quadrant. Thermal demagnetization to 650°C makes no difference in the amount of scatter nor does it alter the mean direction for each site (Fig. 3B). Vector diagrams show a single characteristic magnetization stable up to 625°C, apparently carried by hematite.

In contrast to the redbeds, the basalt exhibits a near-random distribution of NRM vectors. Intensities of NRM are weaker (3×10^{-5}-2×10^{-4} emu/cm^3) than intensities of typical basalts. Thermal demagnetization to 570°C had little effect on the magnetic directions and alternating field demagnetization at 150, 200, and 300 Oe failed to improve the near random distribution of directions. Apparently, the basalt inhomogeneously acquired a number of magnetic components, unlike the single-component magnetization of the nearby redbeds. No useful mean direction could be calculated for the basalt flow.

Ridge Top: Sites 8-12

Upper Triassic redbeds of the central belt crop out on the ridge that divides the drainages of Copeland Creek and Ohio Creek. We collected 25 paleomagnetic samples at 5 sites within the redbeds about 1 km south of the depositional contact between redbeds and the overlying Jura-Triassic sandstones. The redbeds along the spine of the ridge are broken by numerous faults and are folded isoclinally. The sample sites are in 5 fault bounded blocks within the fold's southern limb. Each paleomagnetic site spans about 10 m of stratigraphic section, and the sites are distributed over 200 m of section. Coring was difficult because the rock has been intensely fractured by frost action.

Sites 8, 9, and 10 are in medium and coarse-grained sandstone containing calcareous concretions. The sands are interbedded with stringers of angular red chert pebbles, up to 1 cm in diameter. The redbeds are intruded by several greenish diabase dikes presumably of Tertiary age. Site 11 is in red siltstone marbled on a very fine scale by white calcite veins. Site 12 is 20 m south of the isoclinal fold axis, and consists of coarse red sandstone.

Paleomagnetic results from the Ridge Top

Directions of NRM from the 5 sites are distributed about a steep northerly direction. The intensities of NRM averaged approximately 10^{-5} emu/cm^3. All specimens were thermally demagnetized in steps up to 650°. In general, thermal demagnetization above 400°C recovered a characteristic magnetization that varied little from the direction of NRM, so directional scatter of the data was not significantly improved by the thermal treatment. As was found at Long Creek, the tilt corrections noticeably increased the amount of directional scatter, indicating the magnetization was acquired after folding (Fig. 3C).

Christy Creek: Sites 13-15.

The near-vertical beds exposed in Christy Creek consist of medium-grained red sandstone and pebble-conglomerate. Cross-bedding and filled channels indicate the beds are overturned 5-15 degrees to the south. Thirty-one oriented cores were collected from the water-smoothed banks of the stream at 3 sites, distributed over approximately 100 m of section. Each site spans a stratigraphic thickness of approximately 15 m.

<u>Paleomagnetic results from Christy Creek</u>

NRM directions were scattered about a steep northerly direction similar to the results from the Ridge Top. However, thermal demagnetization revealed a family of directions unlike any other found in redbeds of the Chulitna terrane (Fig. 3D). During thermal treatment the magnetic directions moved toward shallower, more westward directions. The tilt corrections shifted the site means to the southern hemisphere, but did not improve the large dispersion of site means. Vector diagrams from the demagnetization experiments indicate multicomponent magnetizations that may account for the large directional dispersion within sites and the large dispersion between site means. Many specimens heated to 675°C did not reach a stable endpoint magnetic direction, indicating the NRM consists of several magnetic components with overlapping blocking temperature spectra.

<u>Metabasalts of the northwestern belt</u>: Site 16

The northwestern structural belt of the Chulitna terrane consists of redbeds underlain by a distinctive banded formation of limestone beds alternating with basalt flows. Fossils in the limestone suggest a Late Triassic age for the limestone-basalt unit. We sampled 7 basalt flows and one sandstone bed in an overturned section exposed for approximately 200 m along a ridge crest. The true stratigraphic thickness of the section is not known, because parts of the section may be repeated along several faults that cross the ridge. Six to nine cores were drilled from individual basalt flows, 5-50 m thick. The flows are interbedded with light gray limestone beds, 5-20 m thick.

The highly fractured flows are most commonly massive, but a few contain pillow structures or pillow breccia mixed with red chert. The dark green metabasalt contains chlorite and epidote indicative of lower greenschist-facies metamorphism. Calcite veins and calcite-filled vesicles are common.

Paleomagnetic results from the metabasalts

The intensities and directions of magnetization are extremely inhomogeneous within individual metabasalt flows. NRM's ranging from 10^{-3}-10^{-5} emu/cm^3 gave widely scattered directions or peculiar bimodal distributions within flows. These results suggest a complex history of magnetization involving the acquisition of several secondary magnetizations.

Detailed demagnetization treatments were applied in an attempt to sort out the multicomponent magnetizations (Fig. 3E). Two samples from each flow were demagnetized in AF's from 25 to 600 Oe, and 4 samples from each flow were thermally demagnetized up to 580°C. Vector diagrams from these experiments revealed four groups of preferred directions. The least stable component, well- developed in about a third of the specimens, is a steep, northerly direction probably due to recently acquired viscous remanent magnetization (NRM). AF treatment above 200 Oe or thermal treatment above 200°C usually removed the VRM. Treatment at higher temperatures and alternating fields isolated three directional groups characterized by shallow inclinations. In some flows all specimens gave directions that fell into one of these groups, but in others the directions were divided between several groups.

The dominant stable group, comprising all specimens from 3 flows plus half of the specimens from another flow, gave northerly declinations and shallow inclinations ranging from -35° to -15°. Stable endpoints in the demagnetization plots of these specimens were usually reached in AF's above 300 Oe or temperatures above $450^{\circ}C$.

Of the remaining data, one flow reached a stable endpoint with a shallow, westerly direction; half of the specimens from one flow reached a stable shallow, easterly direction; and one flow and the sandstone bed had unstable magnetizations. The coercivity spectra and blocking temperature distributions of the three directional groups are so similar that we cannot build a rationale for accepting one group as the primary magnetization and rejecting the others. As shown in Fig. 3E and F, a statistically meaningful average direction cannot be calculated for the Chulitna metabasalts. We conclude that the remaining portion of the original thermoremanence, if any exists at all, has been masked by several secondary components acquired during a long history of metamorphism and deformation.

Curie temperatures of magnetic minerals in the metabasalts were determined with a balance that records strong-field magnetization as a function of temperature (Fig. 4). The samples were heated in nitrogen gas at 1 atmosphere in applied fields of 2000-5000 Oe. Plots of magnetization as a function of applied field indicate saturation occurs between 2000 and 2500 Oe for 5 flows, but the saturation field exceeds 5000 Oe for the remaining flows.

Seventy-five percent of the specimens have Curie temperatures between $570^{\circ}C$ and 580°; Curie temperatures of the remaining specimens range between $505^{\circ}C$ and $555^{\circ}C$. Relatively low saturation fields (2500 Oe) and Curie temperatures near $580^{\circ}C$ indicate the presence of magnetite (Fe_3O_4). The natural remanence of most samples is probably carried by magnetite, because blocking temperatures determined from the corresponding thermal demagnetization data are less than $580^{\circ}C$, with two exceptions. Blocking temperatures exceeding 580°C were noted in two flows that have saturation fields greater than 5000 Oe. Magnetic remanence of these flows is probably carried by hematite. We infer that the flows having low Curie temperatures (505°-555°C) contain titanium-poor titanomagnetite ($Fe_{3-x}Ti_xO_4$, where $0 < x < 0.15$).

Discussion and Conclusions

We have mentioned the failure of fold tests applied to two sample localities, the Ridge Top and Long Creek. We can test whether the post-faulting magnetization found at these 2 localities extends over the entire region by applying a fold test to the combined data of all redbed sites (Fig. 5). Application of the bedding corrections markedly increases the directional scatter of the 14 site means. Some scatter in declination is expected because our simple tilt correction (rotation axis for the correction is the strike of the bedding) cannot retrieve true paleodeclinations from plunging folds or where oblique slip has occurred on faults. However, the large variation observed in inclination cannot be caused by an oversimplified tilt correction, because the paleohorizontal is well-determined by laminated bedding. We conclude the redbeds were remagnetized on a regional scale after the Chulitna terrane was folded and thrusted, sometime after deposition of the Cretaceous flysch exposed in the Chulitna River valley. The regional remagnetization was apparently followed by minor jostling of fault-bounded blocks, as evidenced by the distribution of virtual geomagnetic poles (VGP) calculated from the uncorrected magnetic directions. Each stratigraphic section, such as Long Creek, gives a separate cluster of VGP's compared to VGP's from the neighboring fault-bounded blocks (Fig. 6)

The post-depositional remanence of the Chulitna redbeds resides in hematite, as indicated by high coercivity of remanence and blocking temperatures up to 675°C. Of the possible magnetization processes, we can rule out detrital remanent magnetization (DRM) as the source of remanence, because the fold test is negative. The remaining processes that may account for Chulitna redbed magnetization are: 1) viscous remanent magnetization (VRM) acquired at low temperature during the Brunhes normal polarity epoch. 2) thermoremanence (TRM) acquired at elevated temperatures during regional metamorphism. 3) chemical remanent magnetization (CRM) acquired by the gradual growth of hematite crystals and the pseudomorphic replacement of iron-bearing minerals by hematite. Demagnetization experiments indicate recent-field VRM makes up a small percentage of the remanence, but the thermal stability of remanence of these redbeds is too high to be explained by VRM alone (Dunlop and Stirling, 1977). A high temperature TRM is also unlikely, because metamorphic minerals of low greenschist-facies place an upper unit of about 350°C on heating due to regional metamorphism. However,magnetic domains with high blocking temperatures measured in the laboratory, can be remagnetized at lower temperatures in nature if the heating occurs over millions of years. The likeliest explanation for the Chulitna redbed magnetization is a combination of TRM and CRM acquired at slightly elevated temperatures (150°C-300°C).

The conditions necessary for the creation of the CRM-TRM combination were probably met when the thrust sheets were deeply buried and hot ground water systems were active. A number of small stocks and dikes near the Golden Zone mine suggest rising magma may have created a chemical environment favorable to the formation of CRM (Hawley and Clark, 1974). We do not imply that all hematite in the Chulitna redbeds was created by this process, for surely the red hematite pigment predates the episode of folding. Instead, the hematite domains responsible for the stable remanence probably grew long after the pigment formed, by the gradual replacement of titanomagnetite and ferromagnesian silicates in the volcanic-rich detritus. Apparently, the late Triassic basalts were impervious to the chemical process active in the redbeds, because the basalts still contain magnetite. The absence of mixed polarity magnetizations suggests remagnetization of the Chulitna redbeds occurred during a single normal polarity epoch, perhaps the long normal epoch of the late Cretaceous. Later tectonic movements have altered the VGP's, so the age of remagnetization cannot be inferred from the mean VGP.

Triassic remanent magnetism of the redbeds was lost or never existed, so we cannot infer the early tectonic history of the Chulitna terrane. The exotic nature of the Chulitna terrane was inferred from dissimilarities in its lithostratigraphy compared to neighboring coeval terranes, but unlike Wrangellia, an exotic origin for the Chulitna terrane cannot be substantiated by paleomagnetic methods.

References cited

Dunlop, D. J. and Stirling, J. M., 1977, 'Hard' viscous remanent magnetization (VRM) in fine-grained hematite, Geophys. Res. Lett., v. 4, p. 163-166.

Hawley, C. C. and Clark, A. L., 1974, Geology and mineral deposits of the Upper Chulitna District, Alaska, U.S. Geol. Professional Paper 758-B, 47 p.

Hillhouse, J. W., 1977, Paleomagnetism of the Triassic Nikolai Greenstone, McCarthy Quadrangle, Alaska, Canada. Jour. Earth Sci., v. 14, p. 2578-2592.

Jones, D. L., Silberling, N. J., Csejtey, Jr., Bela, Nelson, W. H. and Blome, C. D., 1979, Age and significance of ophiolite and adjoining rocks in the Upper Chulitna District, South-central Alaska, U.S. Geol. Survey Professional Paper 1121-A, p.

Jones, D. L., Silberling, N. J., and Hillhouse, J. W., 1977, Wrangellia--A displaced terrane in northwestern North America, Canada. Jour. Earth Sci., v. 14, p. 2565-2577.

Table 1. Paleomagnetic results from redbeds of the Chulitna terrane, southcentral Alaska

SITE	SITE LAT	SITE LONG	N	k	α_{95}	I	D	I_c	D_c	θ(°N)	ϕ(°E)
Long Creek	63.19N	210.35E									
1			17	46	5.3	81.3	264.0	15.2	334.5	57.1	177.9
2			6	563	2.8	79.7	246.0	-0.7	321.7	50.9	180.7
3			24	273	1.8	79.9	254.3	1.2	327.2	53.1	177.7
4			16	108	3.6	80.5	230.4	47.9	348.8	49.1	188.5
Blind Creek	63.22N	210.32E									
5			8	145	4.6	53.9	318.6	41.9	94.8	51.6	91.7
6			8	14	15.3	65.0	295.8	35.0	113.1	51.8	126.3
Ridge Top	63.15N	210.23E									
8			6	7	26.8	71.7	47.9	55.1	342.9	65.6	293.8
9			4	74	10.7	75.1	40.1	42.5	28.9	71.8	285.9
10			3	47	18.3	77.3	18.1	31.0	25.6	81.8	274.2
11			7	67	7.4	74.9	353.5	25.2	1.7	86.7	98.0
12			5	78	8.7	75.8	342.1	27.9	344.2	81.9	128.7
Christy Creek	63.13N	210.20E									
13			9	47	7.6	51.8	356.7	30.0	138.0	59.3	35.7
14			14	5	20.8	34.4	305.6	37.6	185.7	32.6	96.0
15			5	6	33.7	34.0	260.7	9.5	198.8	12.5	136.9

Notes: N = number of specimens; k = Fisher precision parameter for directions; α_{95} = 95-percent confidence radius; I, D = inclination and declination, not corrected for bedding; I_c, D_c = inclination and declination corrected for bedding; θ, ϕ = latitude and longitude of VGP.

Figure captions

Figure 1. Paleomagnetic sample localities in the upper Chulitna District.

Figure 2. Progressive decay of vector components during thermal demagnetization of a typical specimen from the redbeds at Long Creek.

Figure 3. Magnetic directions and 95-percent confidence limits before (crosses and diamonds) and after (dots) application of the tilt correction. All symbols lie in lower hemisphere, except open symbols. Triangle denotes present axial dipole field. (A) Long Creek, sites 1-4, (B) Blind Creek, sites 5 and 6. Site 7 omitted. (C) Ridge Top, sites 8-12, (D) Christy Creek, sites 13-15, (E) Metabasalt flows; site 16, uncorrected for bedding tilt, (F) corrected for bedding.

Figure 4. Magnetic properties of Chulitna metabasalt heated in nitrogen gas in an applied field of 2000 oersteds. Curie temperature of this specimen is 575°C.

Figure 5. Mean magnetic directions from redbed sections before and after application of the structural tilt correction. The present axial dipole direction is indicated by a star. All directions lie in lower hemisphere of projection.

Figure 6. Mean virtual geomagnetic poles from redbed sections, not corrected for tilt of the bedding. Numbers indicate sites listed in Table 1.

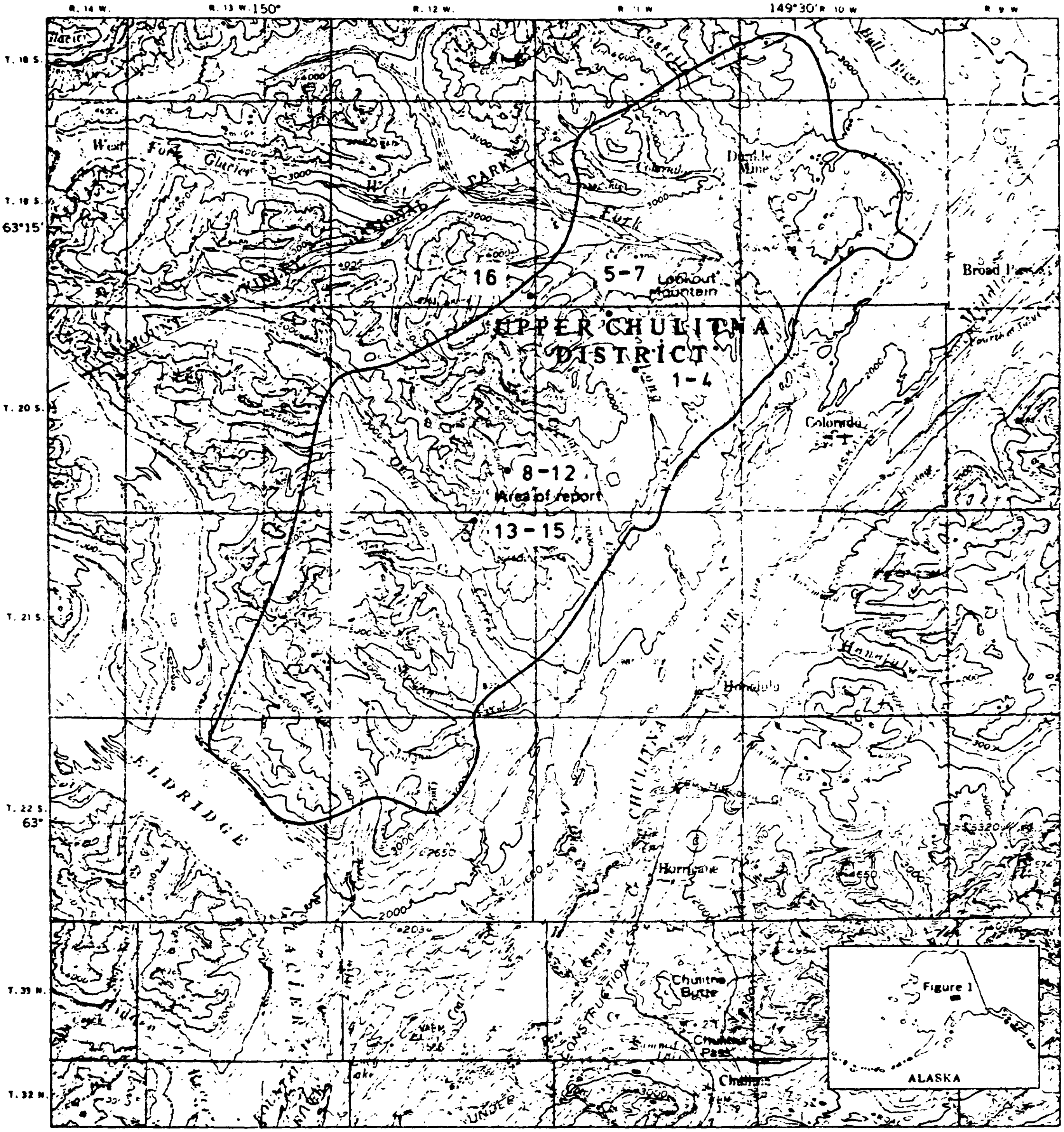

Base from U.S. Geological Survey 1:250 000
Mt. McKinley and Talkeetna, 1958; Healy, 1956;
Talkeetna Mountains, 1954

0 5 10 MILES

0 5 10 KILOMETERS

CONTOUR INTERVAL 200 FEET
DATUM IS MEAN SEA LEVEL

• Paleomagnetic Sites

Fig 1

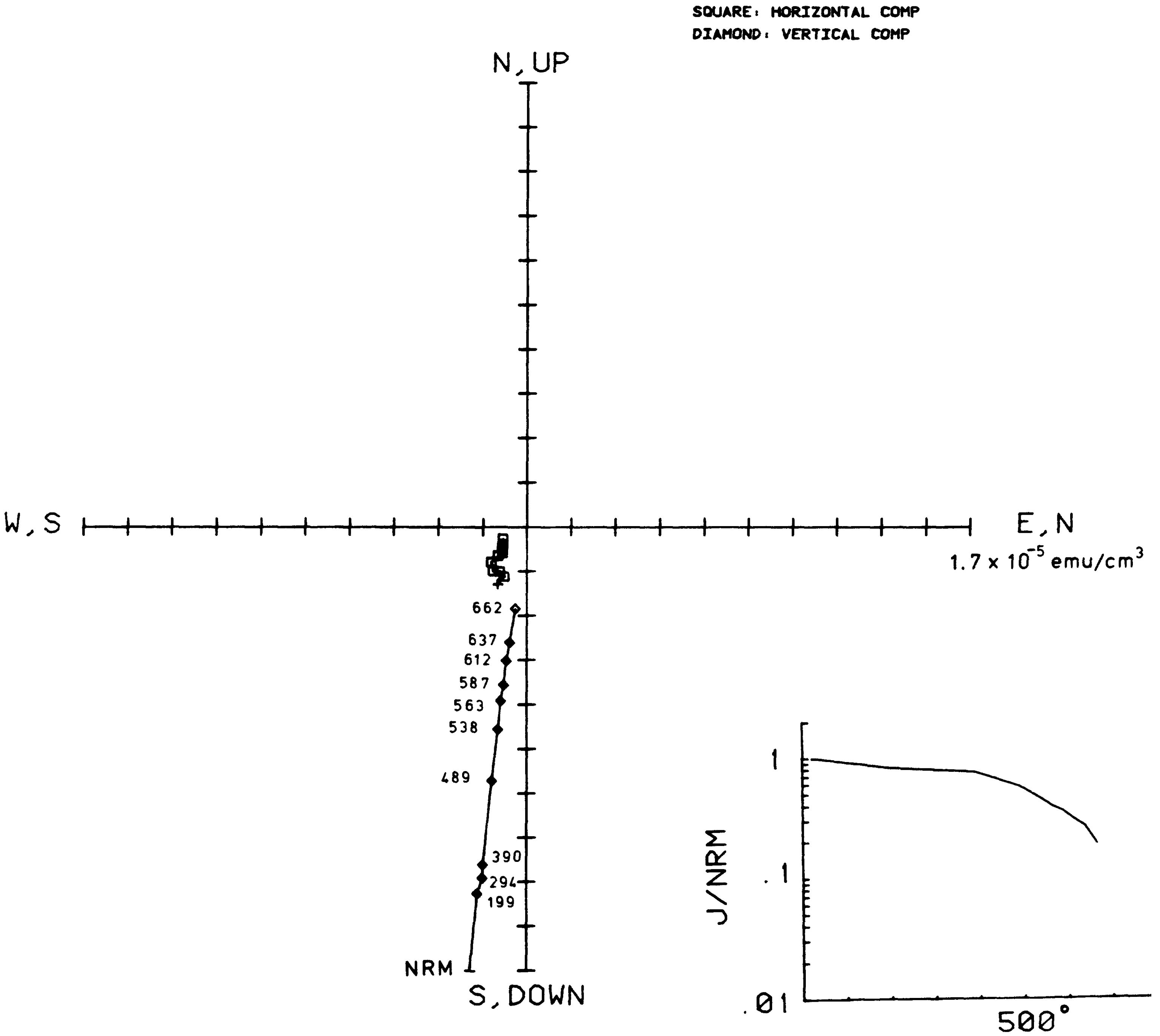
SQUARE: HORIZONTAL COMP
DIAMOND: VERTICAL COMP
N, UP
W, S
E, N
1.7×10^{-5} emu/cm^3
662
637
612
587
563
538
489
390
294
199
NRM
S, DOWN
J/NRM
1
.1
.01
500°

LONG CREEK

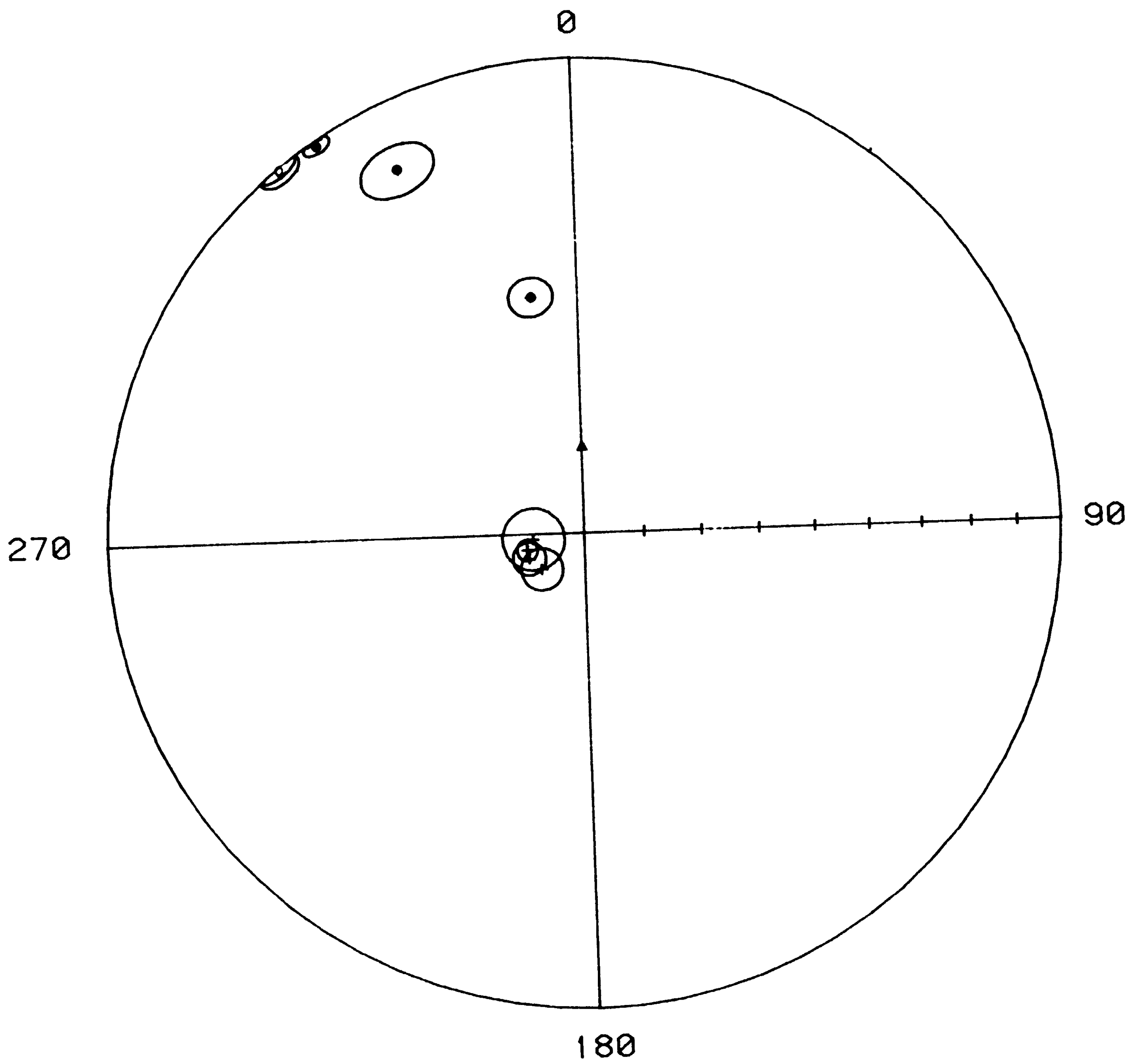

BLIND CREEK

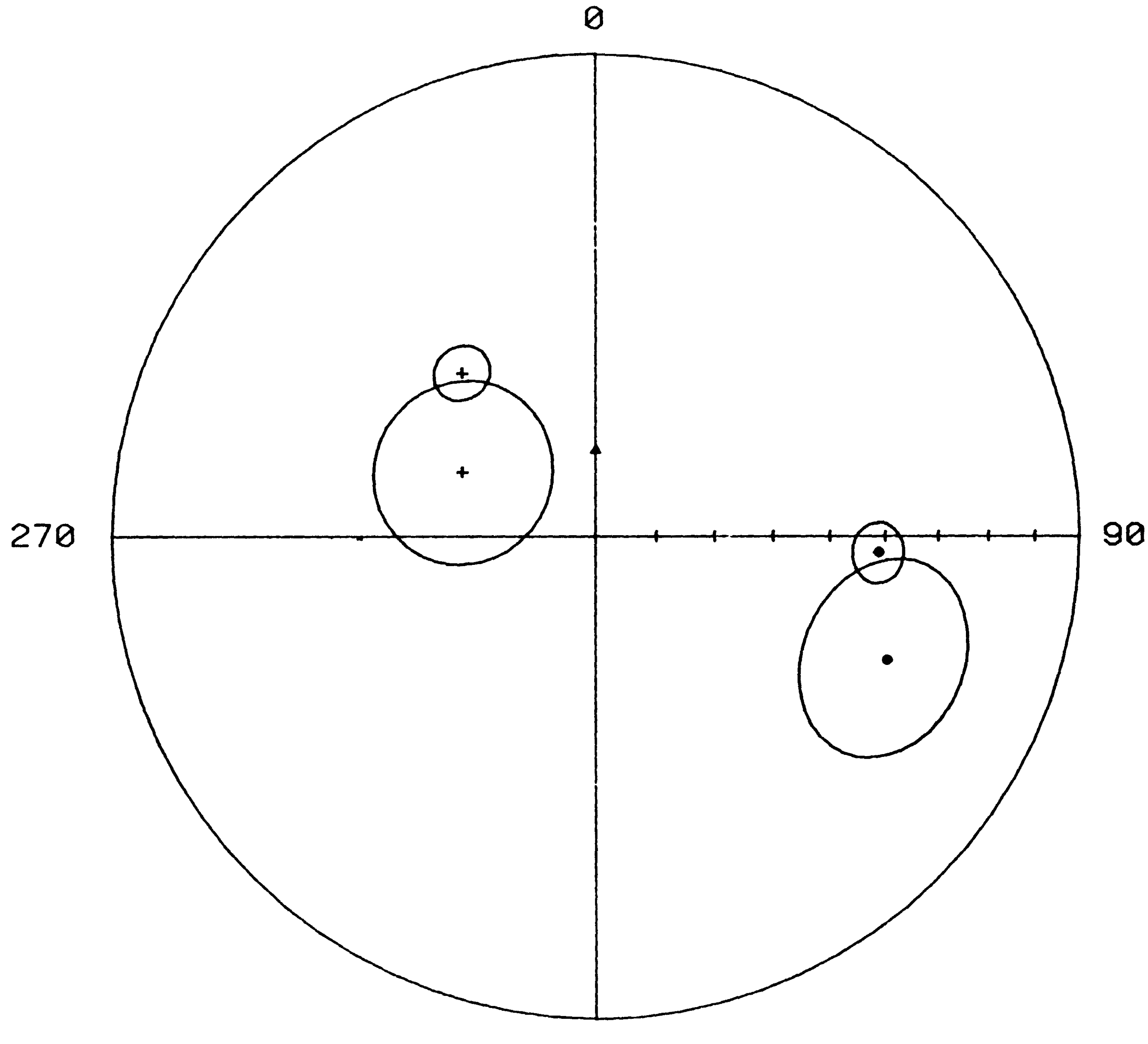

RIDGE TOP

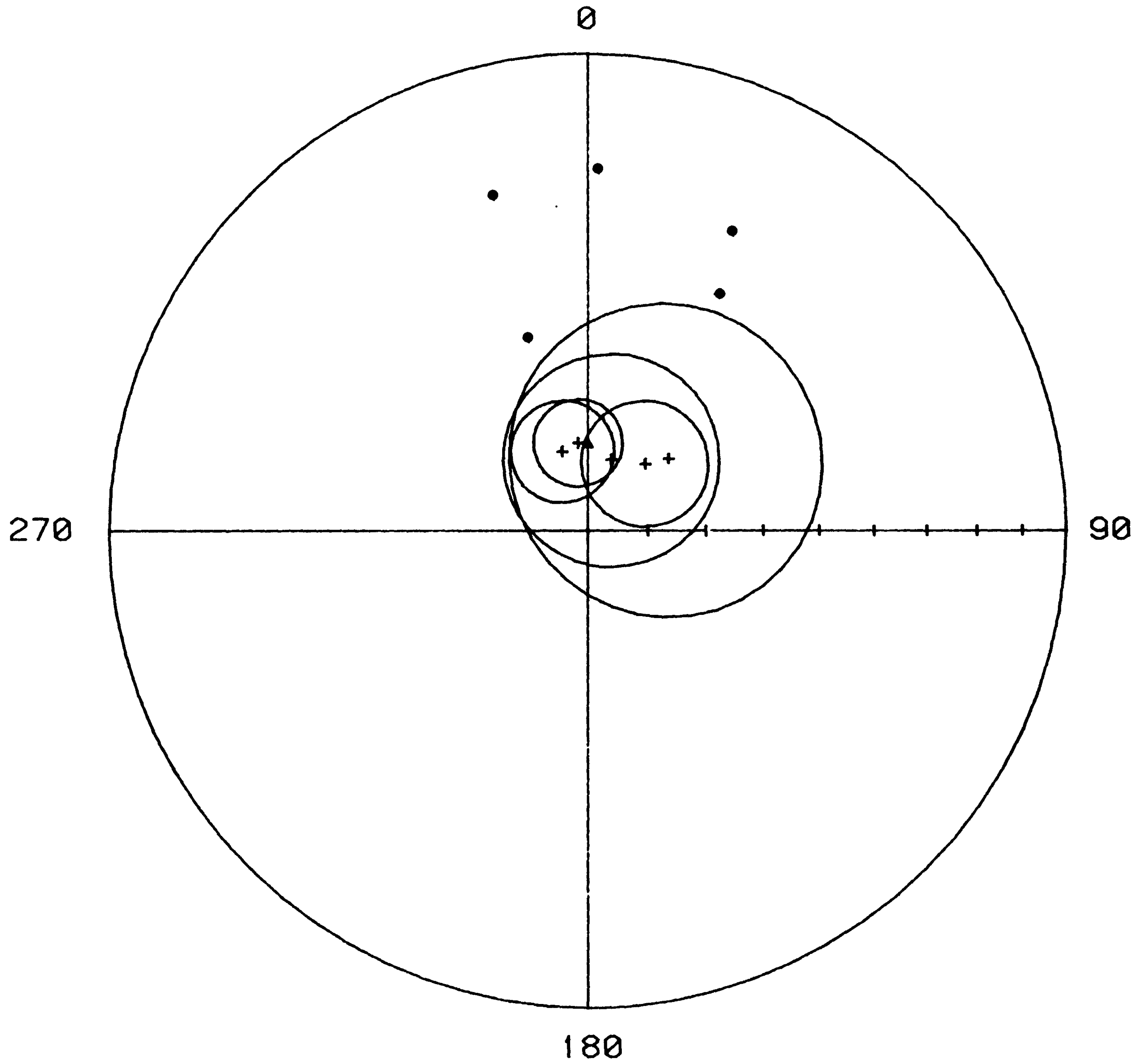

CHRISTY CREEK

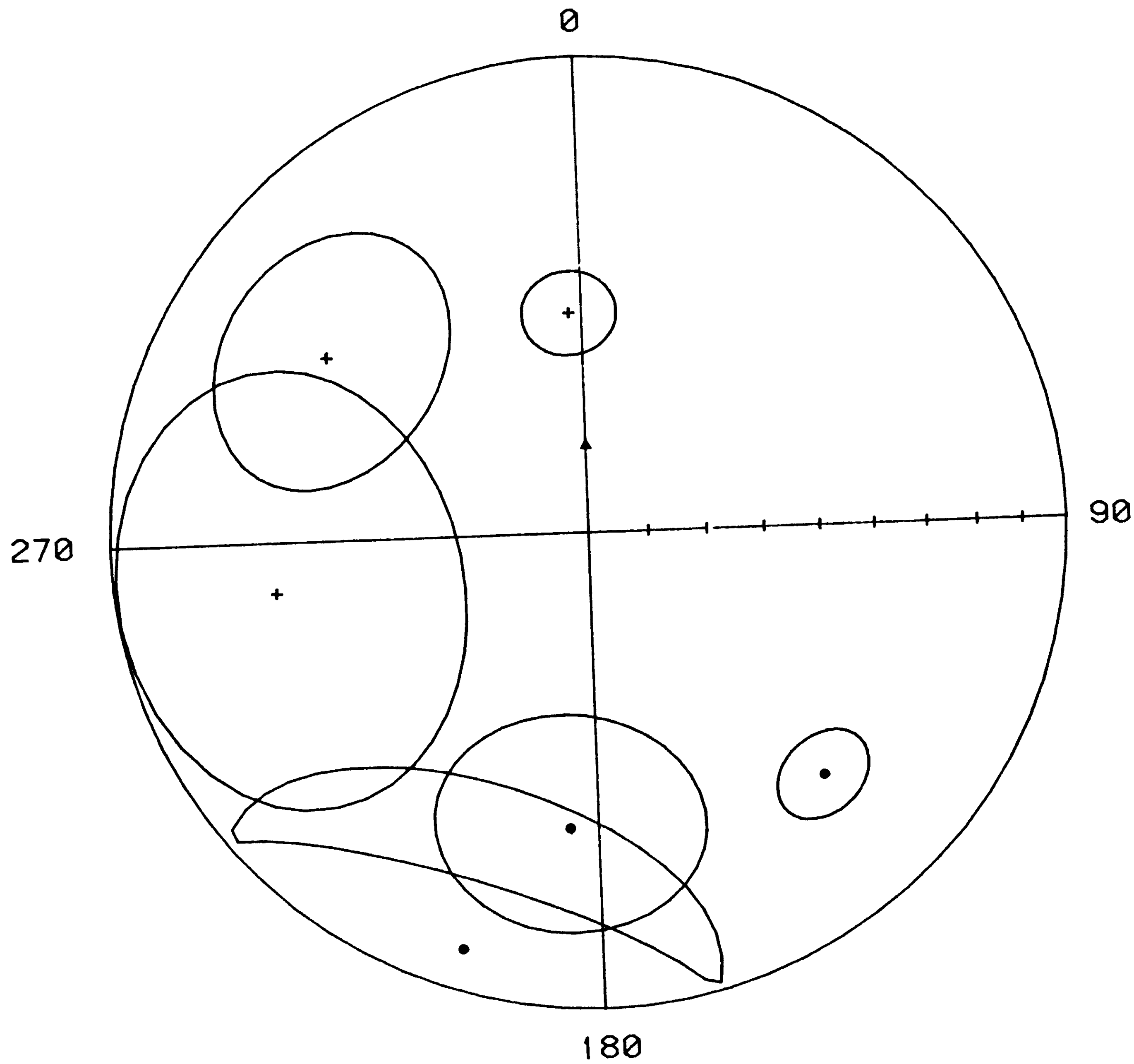

Chulitna Basalts 8K025, 043, 059, 065, 075, 084 Uncorrected 10/3/79

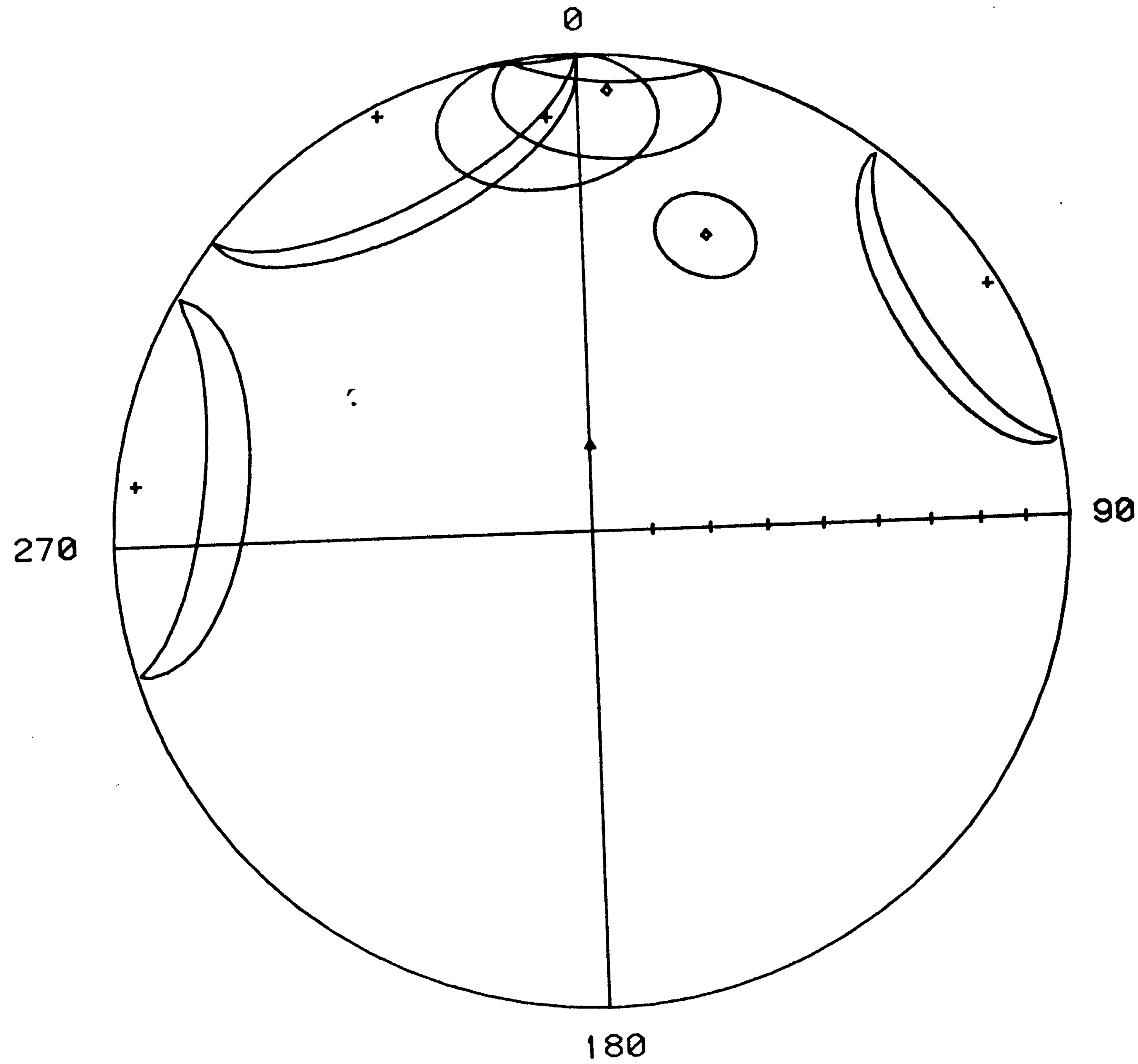

Fig 3E

hulitna Basalts 8K025, 043, 059, 075, 084 Corrected 10/3/79 JH

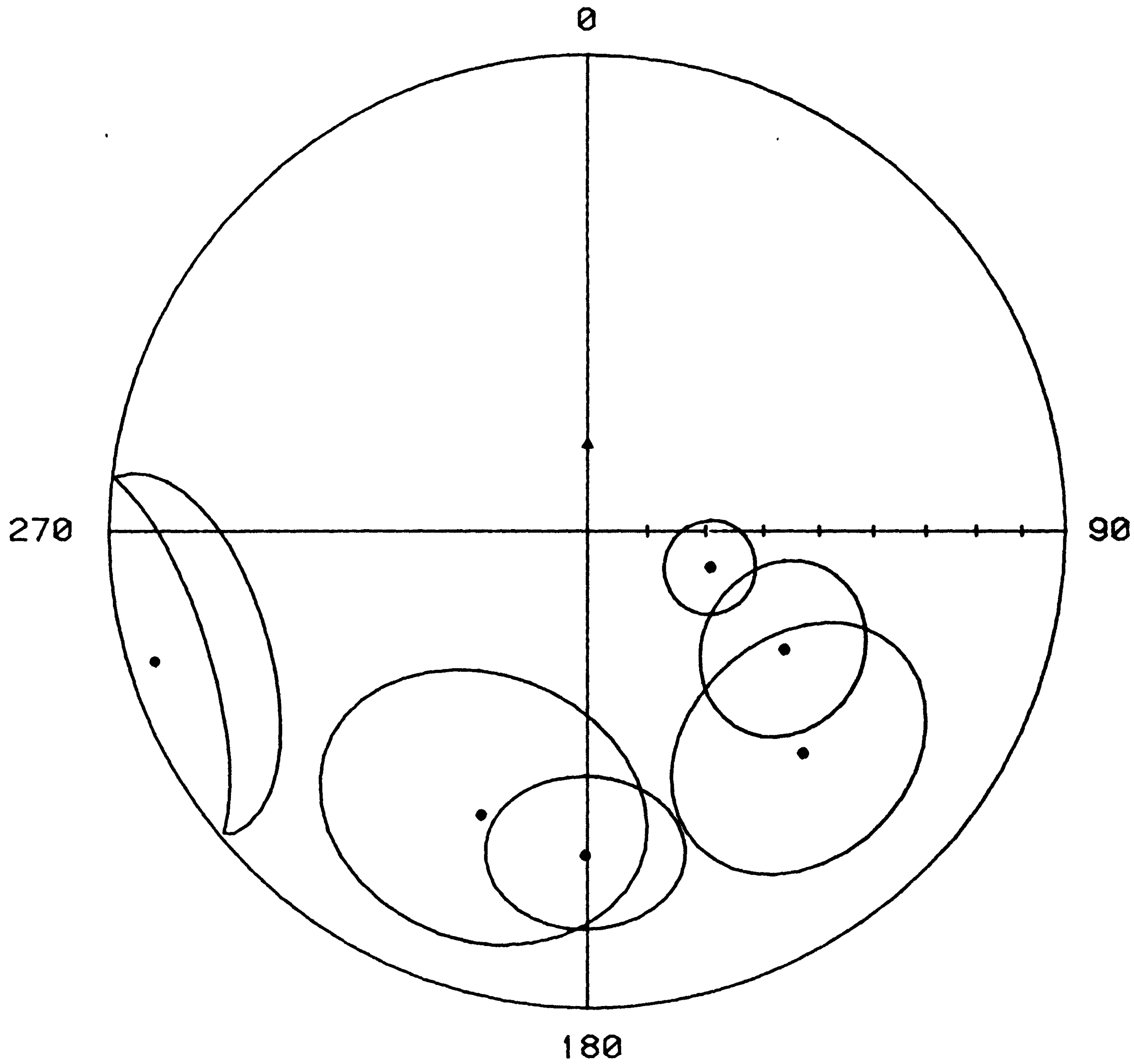

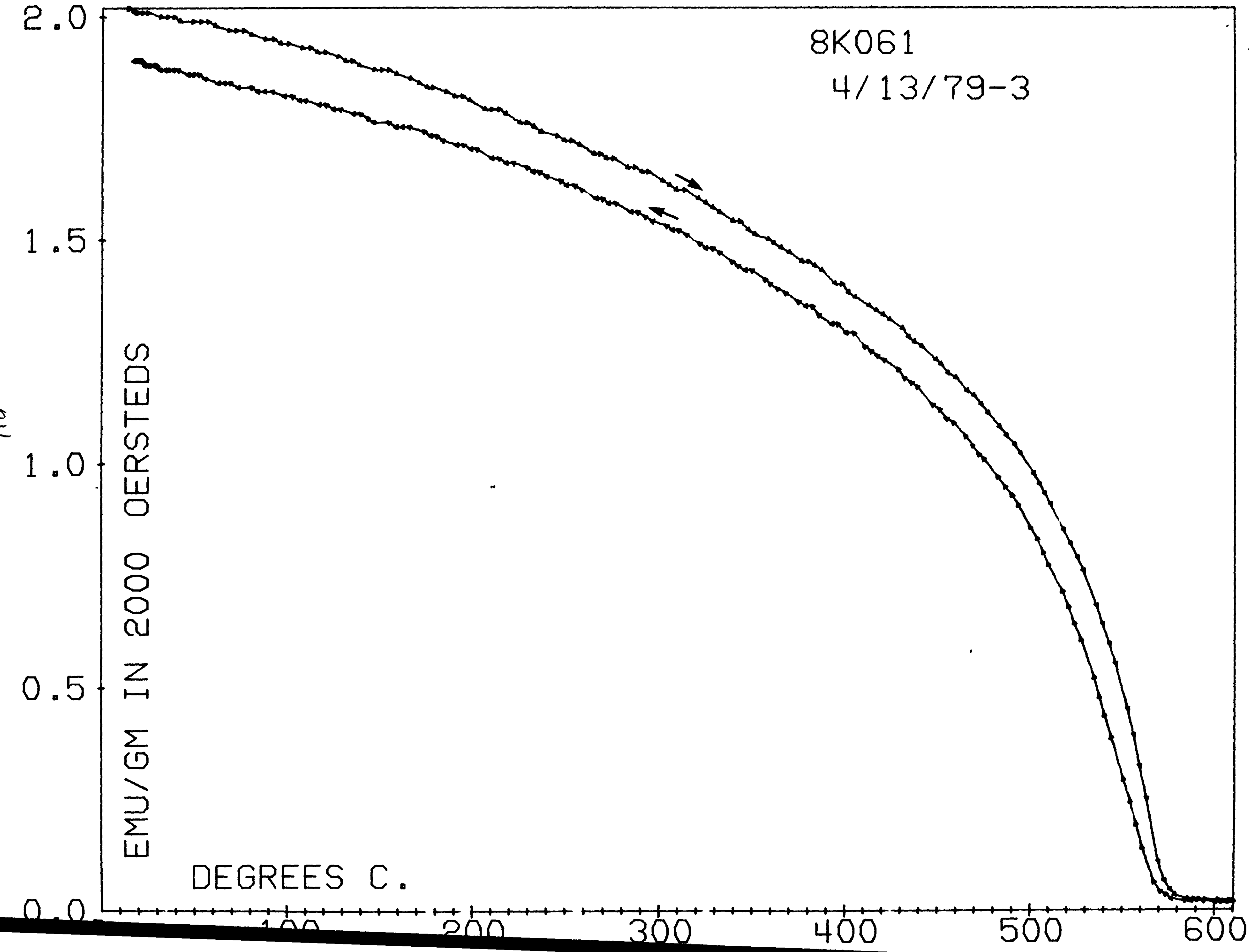

8K061
4/13/79-3
EMU/GM IN 2000 OERSTEDS
DEGREES C.
2.0
1.5
1.0
0.5
0.0
100
200
300
400
500
600

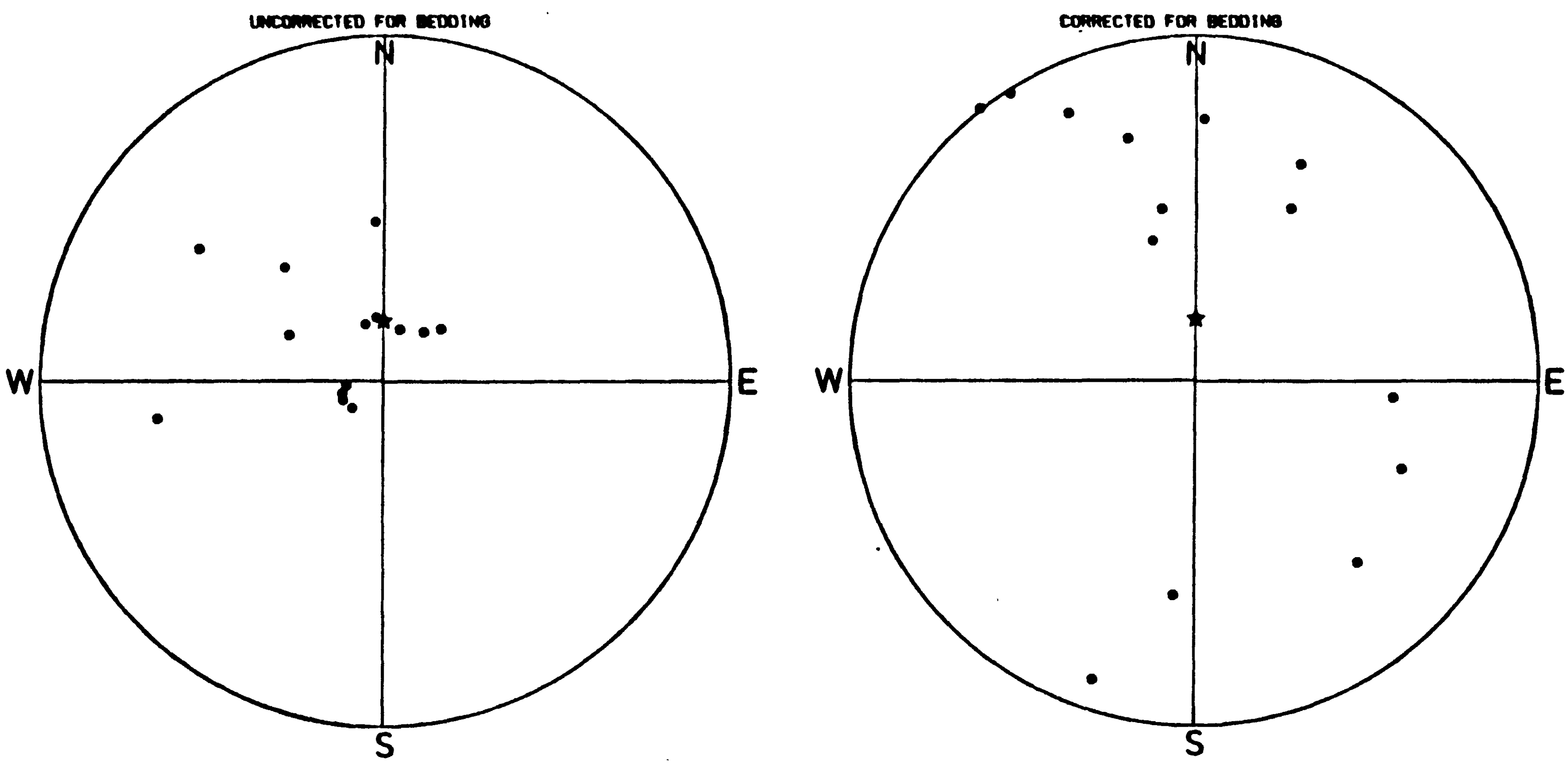

Fig 5.

Fig. 6

CHULITNA RED BEDS--POLES NOT CORRECTED FOR TILT OF BEDDING

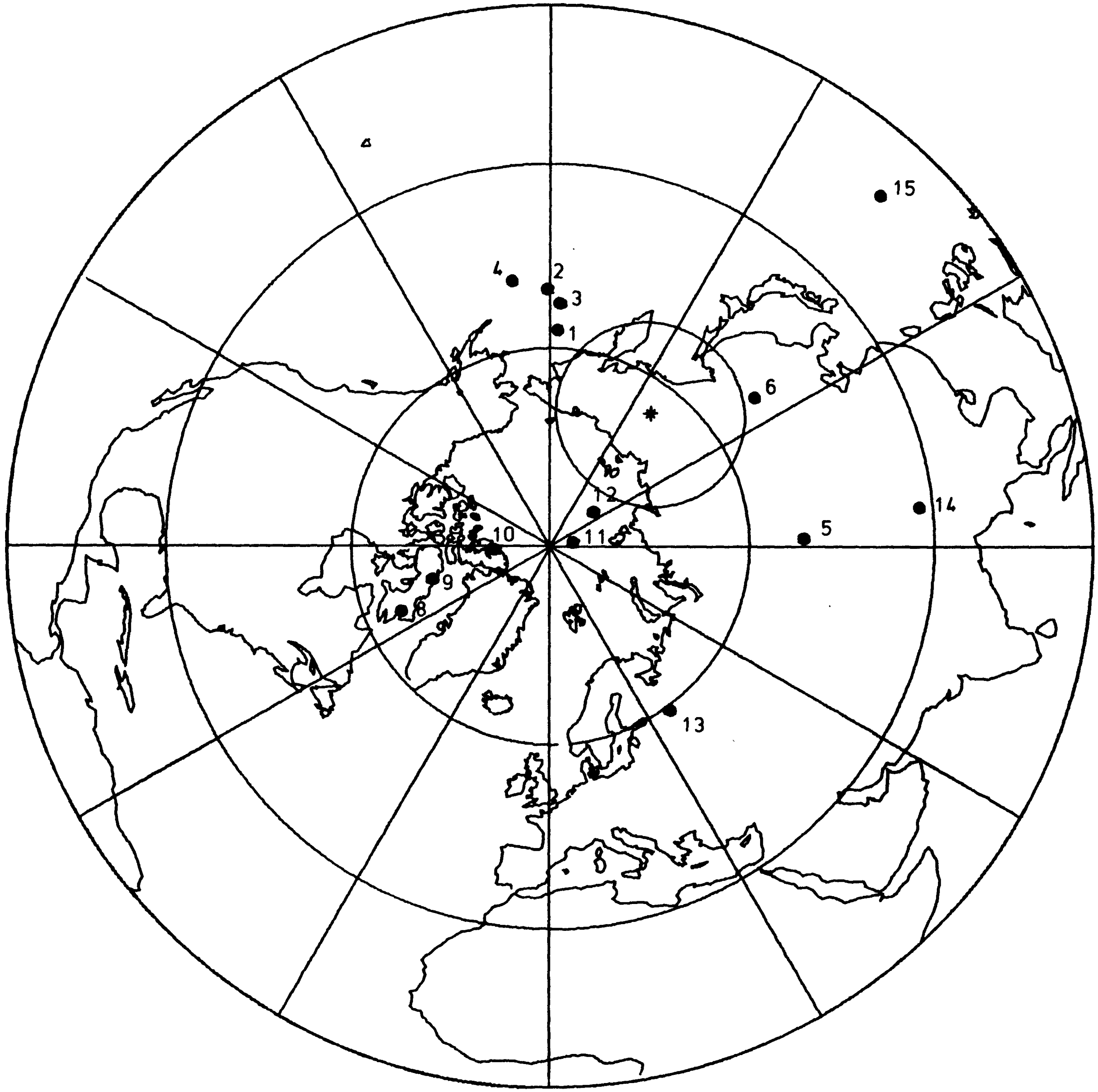

Fig. 6